JOURNAL OF VIETNAM INSTITUTE FOR BUILDING MATERIALS
ISSN 2734 - 9438 ISSN 1859 - 381X
Website: www.jomc.vn

Experimental study on flexural behavior of GFRP reinforced concrete beams

Pham Thi Loan[1], Trinh Duy Thanh[1], Hoang Hieu Nghia[1], Bui Truong Giang[1]

[1] Department of Civil Engineering, Haiphong University, Haiphong, 180000, Vietnam

KEYWORDS

Concrete beam
Flexural behavior
Glass fiber reinforced polymer
Moment resistance
3-point bending test

ABSTRACT

Glass fiber reinforced polymer (GFRP) has been investigated and popularly used as internal reinforcement in the construction field worldwide. Although GFRP is not easy to be corroded, employing it requires an avoidance of the brittle failure mode in order to replace traditional reinforced concrete in designing flexural elements. Therefore, this study brings an incisive view to flexural behavior of concrete beams with GFRP as reinforcements in contribution to apply GFRP to coastal and island construction in Vietnam. This study is based on the tested beams under 3-point bending test and theoretical analysis. The moment resistance of GFRP reinforced concrete beams was designed according to ACI 440-1R code. Materials including GFRP bars and concrete to fabricate tested beams were produced in Vietnam. The investigation reached a conclusion that GFRP is eligible for manufacturing flexural components, which is a potential alternative for traditional concrete in the construction industry.

1. Introduction

Reinforced concrete (RC) is one of the most widely used materials in the construction field. The demand for this material is expected to increase in the future owing to the rise of infrastructure needs in many developing and industrialized countries. Due to the serviceability and economic issues of damaged RC structures by corrosion of the steel bars (GFRP), replacing steel bars with glass fiber-reinforced polymer (GFRP) bars has many advantages. From being innately corrosion resistant, GFRP bars are lightweight, electromechanically neutral, and chemical resistant, as well as having high tensile strength properties [4][8][14].

The flexural behavior of GFRP reinforced concrete beams has been investigated by many researchers around the world (B. Benmokrane, 1996; C. Barris, L. Torres, A. Turon, 2009; Issa et al., 2011; Kumar & Rajkumar, 2016; Maranan et al., 2015; Quang, 2014; Tavares et al., 2008; TCVN5574, 2012) . The results, in general, showed that the behavior of concrete beams reinforced with GFRP bars is different from the traditional RC beams, mainly because of the differences between the physical and mechanical properties of GFRP and steel reinforcements. First, GFRP beams exhibit lower serviceability performance owing to the lower modulus of elasticity of GFRP bars compared to steel bars. Secondly, because concrete crushing failure is less brittle and less catastrophic than GFRP rupture failure due to the rigid and brittle behavior of GFRP bars, GFRP beams are typically built as over-reinforced.. Lastly, since the surface geometries and mechanical features of GFRP bars are different from steel bars, they bond differently to concrete than steel bars. However, the types of rebars available on the market are various and the commercial products are continuously changed. Different fibers are characterized by different behavior under high temperature, environmental effects and long-term phenomena [12].

The durability of GFRP materials has not been yet assessed thoroughly and hence reliable design rules for RC structures are still lacking. Nevertheless, it has been observed that the durability of concrete members reinforced with GFRP rebars depends on the effect of concrete environment for the composite material and cracking and concrete–bar bond. The latter is of paramount importance and depends on the rebar surface adopted by the manufacturer to improve bond (e.g. sanded, ribbed, etc.). Recently, many studies have been carried out on durability of GFRP bars because many aspects influence durability of RC elements with GFRP rebars [2][5][7][11][12]. As mentioned in ACI 440. 1R code (ACI Committee 440, 2015), the values of reduction factors for the flexural strength ranges from 0,55 to 0,65 (Equation 7.2.3 section 7.2.3) in order to avoid both concrete crushing failure and FRP reinforcing bar rupture failure.

This study clarified the failure modes of beams with various GFRP ratios coincided with ACI 440.1R code prediction. Then, ACI 440.1R code was employed for designing moment resistance of glass fiber reinforced concrete beams and the results were appropriate. Besides, the investigation enhances the development of widely applying GFRP to the coastal and island construction in Vietnam as well.

Form the review on the previous studies, the aims of this study are devoted to flexural behavior of beam reinforced with GFRP bars produced in Vietnam. A deep view on the flexural behavior including failure pattern, load-deflection, reduction factors for the moment resistance and strain distributions was analyzed and discussed. In addition, comparisons between test results and code provisions of ACI

https://doi.org/10.54772/jomc.v11i02.290

Received 16/04/2021, explanation 02/07/2021, Accepted 21/07/2021

440.1R were pointed out as well.

2. Test program

Three beams with different GFRP ratios were designed with an adequate amount of longitudinal and shear reinforcement using code provision and tested using 3-point bending test. Details of material, test setup and instrumentation are described below.

2.1 GFRP Bars

As mentioned in the introduction, GFRP bars were provided by Vietnam Glass Fibers Reinforced Polymer Products Joint Stock Company. In this study, GFRP bars with diameter of 8 mm were used and the properties were summarized in Table 1.

Table 1.

Properties of GFRP (Vietnam Fiber Reinforced polymer products joint stock company, 2018).

Outside diameter (mm)	8 ± 0.5	Guaranteed tensile strength f_{fu}^{*} (MPa)	600
Inside diameter (mm)	6 ± 0.5	Elastic modulus (GPa)	46
Area cross section (mm^2)	33.16 ± 2.65	Guaranteed rupture strain ε_{fu}^{*} (%)	2
Density (g/mm)	72 ± 5.76	Thermal coefficient	(4.5-5)x10-6/°C

2.2 Concrete mix proportion

Mixture proportions of concrete with grade of B20 and the characteristics are shown in Table 2 and

Table **3**, respectively.

Table 2.

Mixture proportions of concrete.

Grade	Cement (kg/m^3)	Sand (kg/m^3)	Aggregate (kg/m^3)	Water (kg/m^3)	Water/Cement ratio
B20	405	799	1557	185	0.46

Table 3.

Characteristics of concrete B20.

Grade	Specified compressive strength f_c' (MPa)	Modulus of elasticity of concrete E_c (MPa)	Ultimate strain in concrete ε_{cu}
B20	15	$27.\ 10^3$	$2.\ 10^{-3}$

2.3 Specimen design

The experimental program is implemented based on the beam specimen designed according to the code provision of ACI 440.1R. Three of GFRP reinforced concrete beams were casted using B20 grade of concrete.

The total length of the beam is 1600 mm, with a rectangular cross section of width 100 mm and depth 180 mm. Beams were designed as simple span, with an adequate amount of longitudinal and shear reinforcement to fail by either tensile failure by rupture of GFRP bars or crushing of concrete in the compressive zone as shown detail in Figure 1.

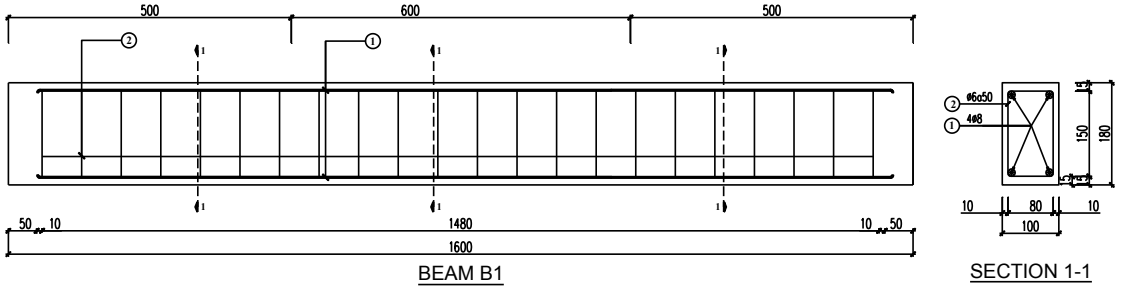

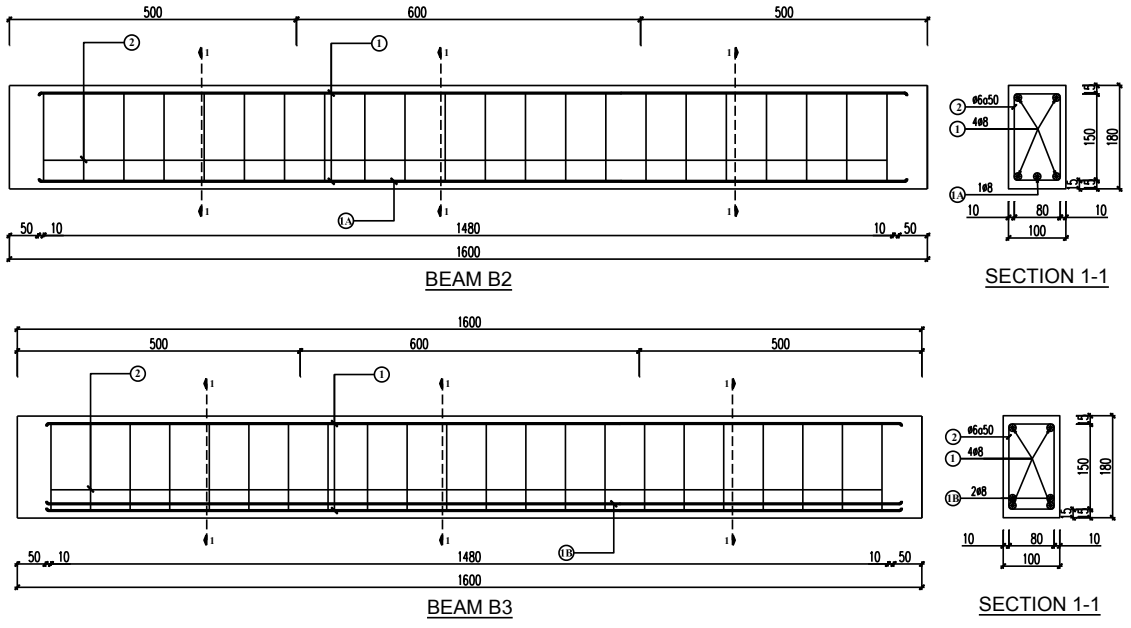

Figure 1. Details of GFRP beams.

These beam specimens were created using the concrete B20's compressive strength and different quantities of GFRP bars in the bottom layer. To prevent shear failure, the shear span is reinforced with enough steel stirrups (6 mm @ 150 mm). Geometric and reinforcement details of the beam are given in

Table **4.**

Table 4.

Details of test specimen designation.

Beam Series	Top – GFRP Reinf.	Bottom – GFRP Reinf.	Steel stirrups
B1	2 # 8 mm	2 # 8 mm	6 mm @ 50 mm
B2	2 # 8 mm	3 # 8 mm	6 mm @ 50 mm
B3	2 # 8 mm	4 # 8 mm	6 mm @ 50 mm

Nominal flexural strength of GFRP beams was calculated according to ACI 440.1R and the results was presented in Table 5.

Table 5.

Nominal flexural strength M_n of GFRP beams.

Beam	b (mm)	d (mm)	A_f (mm^2)	f_{fu} (MPa)	ρ_{fb} (%)	ρ_f (%)	f_f (MPa)	a (mm)	M_n (kNm)
B1	100	151	66.32	420	0.46	0.43	420	21.80	4.01
B2	100	151	99.48	420	0.46	0.64	348.6	27.14	4.90
B3	100	147	132.64	420	0.46	0.90	286.8	29.77	5.03

Note: b is the width of rectangular cross section;

d is the distance from extreme compression fiber to centroid of tension reinforcement;

A_f is area of fiber-reinforced polymer reinforcement;

f_{fu} is the design tensile strength of GFRP considering reductions for service environment.

$$f_{fu} = C_E f^*_{fu}$$

C_E is an environmental reduction factor taken 0.7; f^*_{fu} is guaranteed tensile strength of GFRP bar taken 600MPa according to *Factory Standard TC01:2018/FRP Vietnam* (Vietnam Fiber Reinforced polymer products joint stock company, 2018).

f_f is the stress in GFRP reinforcement in tension;

ρ_f is GFRP reinforcement ratio:

$$\rho_f = \frac{A_f}{bd} \quad \text{(E2)}$$

ρ_{fb} is GFRP reinforcement ratio producing balanced strain conditions:

$$\rho_{fb} = 0.85\beta_1 \frac{f'_c}{f_{fu}} \frac{E_f \varepsilon_{cu}}{E_f \varepsilon_{cu} + f_{fu}} \quad \text{(E3)}$$

β_1 was taken equal to 0.85 for f'_c below 28MPa and ε_{cu} was taken equal to 0.2 %.

M_n is the nominal flexural strength:

If $\rho_f \leq \rho_{fb}$ then M_n:

$$M_n = A_f f_{fu} . (d - \frac{a}{2}) \quad \text{(E4)}$$

If $\rho_f > \rho_{fb}$ then M_n:

$$M_n = A_f . f_f . (d - \frac{a}{2}) \quad \text{(E5)}$$

$$f_f = \sqrt{\frac{E_f \varepsilon_{cu}}{4} + \frac{0.85\beta_1 f'_c}{\rho_f}} E_f \varepsilon_{cu} - 0.5 E_f \varepsilon_{cu} \quad \text{(E6)}$$

$$a = \frac{A_f f_f}{0.85 f'_c b} \quad \text{(E7)}$$

The value of specified compressive strength of concrete grade B20, $fc' = 15$ MPa was adopted. The tested beams were subjected to static load until failure, reduction factors for the flexural strength were not taken in to account the flexural strength of GFRP beams.

2.4 Specimen fabrication

These specimens were fabricated in the laboratory at Haiphong University. Firstly, reinforcing bars of both components were assembled into the reinforcing cages. Then the reinforcing cages were moved to the platforms that were used as the base forms, the wooden forms were coated with oil. All of the components were prepared for being moulded. Ready-mix concrete grade of B20 was used for all the specimens. Finally, the specimens casted were cured at ambient temperature for 28 days as shown in Figure 2.

a) Reinforcing cages located in the wooden form

b) Pouring ready-mix concrete

c) Specimens casted and cured

Figure 2. Specimen fabricated.

2.5 Experimental setup and loading

The experimental beams with nominal length of 1400 mm and loaded by 3-point bending test. Each specimen was supported on roller assemblies in order to locate the exact supporting point. In order to measure the deflection based on the load applied the linear variable differential transformers (LVDT) were used to record the deflection. LVDT was fixed at mid-section of the beam specimen - under the loading point and four strain gauges embedded over the height of beams to record the strain of concrete. The test setup and instrumentations for tested specimens are illustrated in Figure 3 and captured in Figure 4.

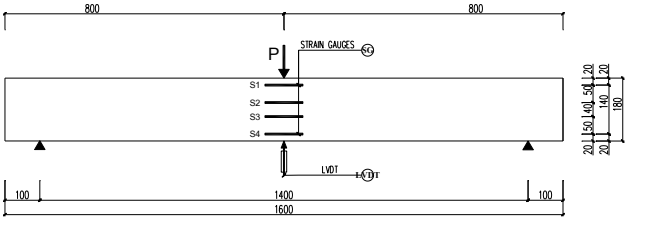

Figure 3. Scheme of LVDT and strain gauges on tested beams.

Figure 4. Specimen setup before loading.

The values of design ultimate load were obtained from this formular:

$$P_{max}^{design} = \frac{4M_n}{l} \quad \text{(E8)}$$

where M_n is the nominal flexural strength which was determined in Table 5; l is the clear span of the beam.

Loading process was based on TCVN 9374:2012. According to TCVN 9374:2012, every load increment was lower than 10% of value load corresponding to strength designed of the specimen. The tested loads were increased until the final stage of test and the values were recorded as shown in Table 6.

Table 6.
Maximum tested loads.

Beam Series	M_n (kNm)	P_{max}^{design} (kN)	P_{max}^{test} (kN)	Difference (%)
B1	4.01	11.4	11.46	0.5
B2	4.90	14	14.38	2.7
B3	5.03	14.4	14.4	0

3. Results and discussions

In this section, the most significant results are presented using several theoretical approaches.

3.1 Cracking and failure modes

The flexural capacity of an GFRP - reinforced flexural member is dependent on whether the failure is governed by concrete crushing or GFRP rupture as shown in Figure 5.

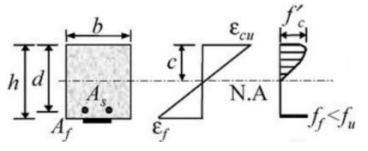

a) Failure governed by concrete crushing

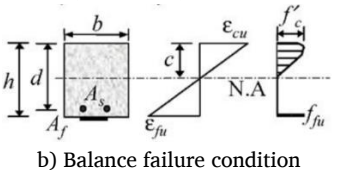

b) Balance failure condition

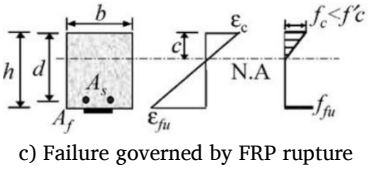

c) Failure governed by FRP rupture

Figure 5. Strain and stress distribution at ultimate conditions.

The failure mode can be determined by comparing the FRP reinforcement ratio to the balanced reinforcement ratio ρ_{fb} to ρ_f, then the failure is governed by concrete crushing or FRP rupture.

When $\rho_f > \rho_{fb}$, the failure of the member is initiated by crushing of the concrete otherwise, the failure of the member is initiated by rupture of FRP bar. In this study, specimen B2 and B3 was designed in order to subjected to ultimate load with the failure of crushing of the concrete but the specimen B1 was failure with the rupture of FRP bar as shown in Figure 6. The difference between designed load and tested load of the specimen B1 is smallest as illustrated in Table 6. It indicates that the reserve of strength in the member is limited and critical.

Table 7.
The stress in GFRP reinforcements in tension at the final load.

Beam	Ultimate load (kN)	ρ_{fb} (%)	ρ_f (%)	Failure modes
B1	11.46	0.46	0.43	GFRP rupture
B2	14.38	0.46	0.64	Concrete crushing
B3	14.4	0.46	0.90	Concrete crushing

(a) Beam B1

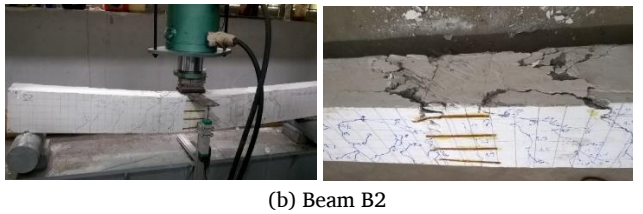

(b) Beam B2

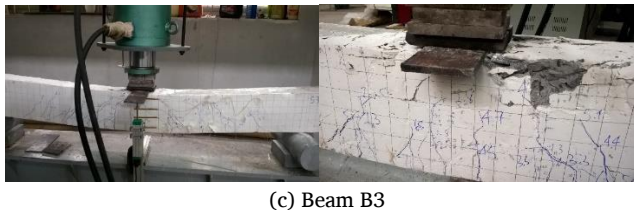

(c) Beam B3

Figure 6. Failure modes of GFRP beams.

During the test, the cracks on the beams were observed visually from the first crack appeared and to failure corresponding loads recorded. The first crack appeared with the load values of cracking curves was 1.6 kN, 1.8 kN and 3.8 kN in the sequence of beam B1, B2 and B3, respectively.

The vertical flexural cracks distributed relatively regular on the middle zone of beam of beam B1. After some stages of loading the cracks were propagated and extended. The B1 beam was destroyed due to GFRP rupture in the tensile concrete area as proved in **Table 7**, while concrete in the compression zone were also crushed as shown in Figure 6 (a). There were almost no inclined cracks on the beam B1. Beams B2 and B3 are similarly cracks propagated. Vertical flexural cracks are mainly concentrated near the load point while cracks spreading to the side of the supports tended to incline. It can be seen that the concrete in the compression zone of GFRP reinforced beams were seriously crushed as shown in Figure 6 (b) and (c).

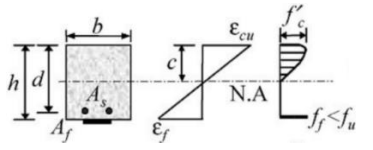

a) Failure governed by concrete crushing

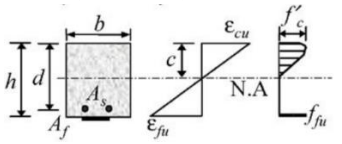

b) Balance failure condition

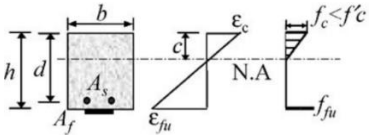

c) Failure governed by FRP rupture

Figure 5. Strain and stress distribution at ultimate conditions.

3.2 Load-deflection curves

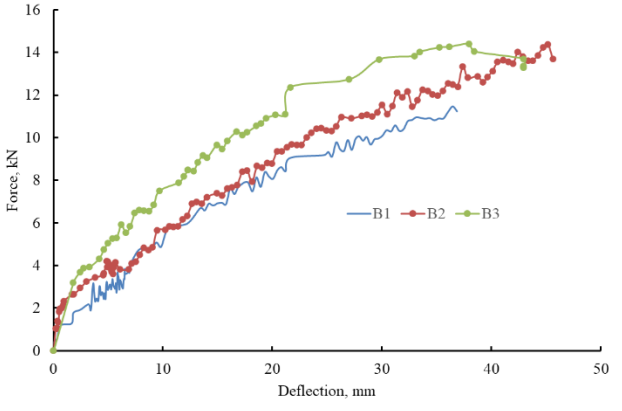

Figure 7. Load-deflection relationship of GFRP beams.

The load-deflection curves of GFRP reinforced concrete beams are presented in Figure 7. Each curve represents the deflection readings obtained from the LVDT at the mid-span. The load - deflection curves consist primarily of two linear segments. The first linear branch that corresponds to cracked response of the beam denoted by C1, C2 and C3 points corresponding to B1, B2 and B3 respectively; and the second linear segments with reduced slope that represent the cracked response of the beam and stiffness degradation denoted by the rested line after C1, C2 and C3 points corresponding to B1. B2 and B3 respectively. The characteristic of the curves obtained from this study is similar to that of previous research by other authors [2].

3.3 Strength reduction factor for flexure

The biggest disadvantages of FRP members is not exhibiting ductile behavior, so a conservative strength reduction factor should be adopted to provide a higher reserve of strength in the member. According to ACI 440.1 R, the strength reduction factor ϕ was set to 0.65 for concrete crushing failure, and 0.55 for FRP reinforcing bar rupture failure. The factor ϕ as a function of the reinforcement ratio is expressed in the equation (E9) and Figure 8.

$$\phi = \begin{cases} 0.55 & for\ \rho_f \le \rho_{fb} \\ 0.3 + 0.25\dfrac{\rho_f}{\rho_{fb}} & for\ \rho_{fb} < \rho_f < 1.4\,\rho_{fb} \\ 0.65 & for\ \rho_f \ge 1.4\rho_{fb} \end{cases}$$

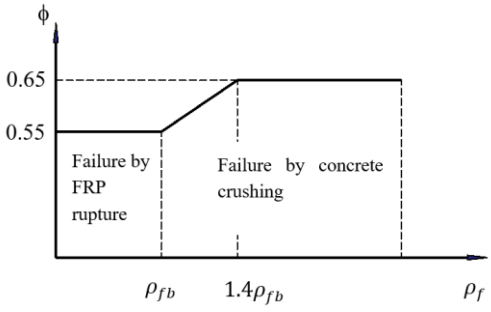

Figure 8. Variation of the strength reduction factor.

Table 8.

Allowed loads corresponding the strength reduction factor ϕ.

Beam	A_f (mm^2)	ρ_{fb} (%)	ρ_f (%)	ϕ	ϕM_n (kNm)	Allowed load (kN)
B1	66.32	0.46	0.43	0.55	2.21	6.31
B2	99.48	0.46	0.64	0.64	2.62	7.49
B3	132.64	0.46	0.90	0.65	3.27	9.34

The designed specimens were tested up to the ultimate load and the failure modes are well matched with the distinguishing by ACI 440.1R as presented in Table 5. Therefore, to provide a safety at the service stage of element, the strength reduction factor ϕ needs to be taken to account the nominal flexural strength. In another words, the load subjected to the specimens must be scaled down with the strength reduction factor ϕ and the results are given in Table 8.

3.4 Strain distribution

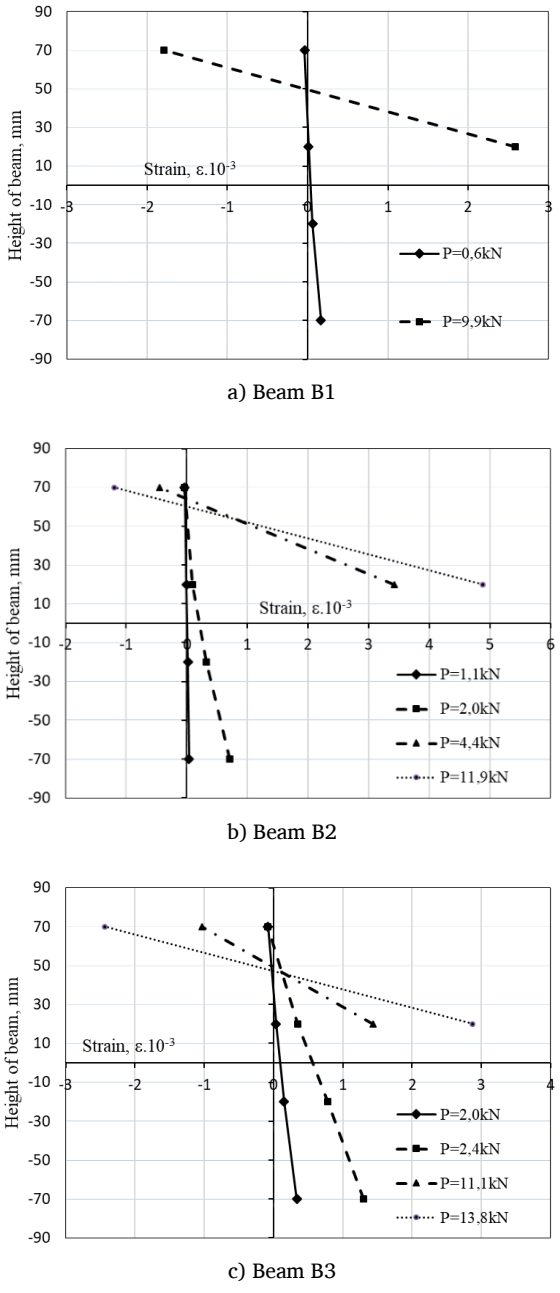

a) Beam B1

b) Beam B2

c) Beam B3

Figure 9. Distribution of strain along the height of GFRP beams.

The distributions of strains on the cross-section of GFRP beams are drawn according to the reading from the strain gauges attached along the height as shown in. The typical strain distributions of tested beams B1,, B2 and B3 are displayed in Figure 9, respectively. It is clear from the figures that prior to cracking. the distribution of the strains on the cross-section of beams almost varies linearly along the height of the beam. After cracking only compressive strains were drawn because the contributions of the concrete in the tension zone were ignored. Based on the results. it can be summarized that the plane section assumption remains valid in application for GFRP reinforced concrete beams.

4. Conclusions

Flexural behaviors of GFRP reinforced concrete beams were investigated experimentally and theoretically. The following conclusions are given within the limit of the present study:

(1) The design provisions of ACI.1R were appropriately employed to determine the flexural strength of GFRP reinforced beams with materials including GFRP bars and concrete produced in Vietnam.

(2) Failure modes of GFRP beams obtained by test were coincided with theory of ACI.1R.

(3) The load–deflection curves of the RC beams with GFRP bars consist primarily of two linear segments, including a linear branch that corresponds to cracked response of the beam; and linear segments with reduced slope that represent the cracked response of the beam and stiffness degradation.

(4) The range (0.55-0.65) of strength reduction factor for flexural strength plays an important role to ensure the resistance of beams and to avoid both concrete crushing and FRP rupture failure in the service stage.

(5) The plane section assumption remains valid in application for GFRP reinforced concrete beams.

Acknowledgement

This work was sponsored by Haiphong University. The authors would like to thank Vietnam Glass Fibers Reinforced Polymer Products Joint Stock Company for providing GFRP.

References

[1] ACI Committee 440. (2015). ACI 440.1R-15 Guide for the design and construction of structural concrete reinforced with Firber-Reinforced Polymer (FRP) bars. In *American Concrete Institute (ACI)*.

[2] Alsayed, S. H., Al-Salloum, Y. A., & Almusallam, T. H. (2000). Performance of glass fiber reinforced plastic bars as a reinforcing material for concrete structures. *Composites Part B: Engineering*, *31*(6–7), 555–567. https://doi.org/10.1016/S1359-8368(99)00049-9

[3] B. Benmokrane, O. C. and R. M. (1996). Flexural Response of Concrete Beams Reinforced with FRP Reinforcing Bars. *ACI Struct. J.*, *91*(2), 46–55.

[4] Balsamo, A., Coppola, L., & Zaffaroni, P. (2001). FRP in Construction: Applications, Advantages, Barriers and Perspectives. *Composites in Construction*, 58–64. https://doi.org/10.1061/40596(264)7

[5] Bank, L. C., Gentry, T. R., & Barkatt, A. (1995). Accelerated Test Methods to Determine the Long-Term Behavior of FRP Composite Structures: Environmental Effects. *Journal of Reinforced Plastics and Composites*, *14*(6), 559–587. https://doi.org/10.1177/073168449501400602

[6] C. Barris, L. Torres, A. Turon, M. B. and A. C. (2009). An Experimental Study of the Flexural Behavior of Gfrp Rc Beams and Comparison With Prediction Models. *Int. J. Composite Mater.*, *91*(13), 286–295.

[7] Ceroni, F., Cosenza, E., Gaetano, M., & Pecce, M. (2006). Durability issues

of FRP rebars in reinforced concrete members. *Cement and Concrete Composites*, *28*(10), 857–868. https://doi.org/10.1016/j.cemconcomp.2006.07.004

[8] Einde, L. Van Den, Zhao, L., & Seible, F. (2003). Use of FRP composites in civil structural applications. *Construction and Building Materials*, *17*, 595–602. https://doi.org/10.1016/S0950-0618

[9] Reinforced concrete and prefabricated concrete building products - Loading test method for assenssment of strength, rigidity and crack resistance, (2012).

[10] Issa, M. S., Metwally, I. M., & Elzeiny, S. M. (2011). Influence of fibers on flexural behavior and ductility of concrete beams reinforced with GFRP rebars. *Engineering Structures*, *33*(5), 1754–1763. https://doi.org/10.1016/j.engstruct.2011.02.014

[11] Karbhari, V. M. (2003). Durability of FRP Composites for Civil Infrastructure — Myth, Mystery or Reality. *Advances in Structural Engineering*, *6*(3), 243–255. https://doi.org/10.1260/136943303322419250

[12] Kim, H.-Y., Park, Y.-H., You, Y.-J., & Moon, C.-K. (2006). Durability of GFRP composite exposed to various environmental conditions. *KSCE Journal of Civil Engineering*, *10*(4), 291–295. https://doi.org/10.1007/BF02830783

[13] Kumar, D. S., & Rajkumar, R. (2016). Experimantal investigation on flexural behavior of concrete beam with glass fiber reinforced polymer rebar as internal reinforcement. *Int. J. Chem. Sci.*, *14*, 319–329.

[14] Ma, M. L., Wang, G. L., Miao, D. M., & Xian, G. J. (2013). A Review on Engineering Application of FRP Material: Case Study and Practice. *Advanced Materials Research*, *800*, 308–311. https://doi.org/10.4028/www.scientific.net/AMR.800.308

[15] Maranan, G. B., Manalo, A. C., Benmokrane, B., Karunasena, W., & Mendis, P. (2015). Evaluation of the flexural strength and serviceability of geopolymer concrete beams reinforced with glass-fibre-reinforced polymer (GFRP) bars. *Engineering Structures*, *101*, 529–541. https://doi.org/10.1016/j.engstruct.2015.08.003

[16] Quang, N. V. N. (2014). *Optimizing the calculation of longitudinal reinforcement of GFRP fiberglass reinforced concrete beams according to ACI 440.1R.2006*. Danang University.

[17] Tavares, D. H., Giongo, J. S., & Paultre, P. (2008). Behavior of reinforced concrete beams reinforced with GFRP bars. *IBRACON Structures and Materials*, *1*(3), 285–295.

[18] TCVN5574. (2012). *Concrete and reinforced concrete structures - Design standard*.

[19] Vietnam Fiber Reinforced polymer products joint stock company. (2018). *Factory Standard TC01:2018/FRP Vietnam*.